The Structural Bases of Antibiotic Resistance in the Clinically Derived Mutant β-Lactamases TEM-30, TEM-32, and TEM-34*

Xiaojun Wang‡, George Minasov‡, and Brian K. Shoichet§

From the Department of Molecular Pharmacology and Biological Chemistry, Northwestern University, Chicago, Illinois 60611-3008

Widespread use of β-lactam antibiotics has promoted the evolution of β-lactamase mutant enzymes that can hydrolyze ever newer classes of these drugs. Among the most pernicious mutants are the inhibitor-resistant TEM β-lactamases (IRTs), which elude mechanism-based inhibitors, such as clavulanate. Despite much research on these IRTs, little is known about the structural bases of their action. This has made it difficult to understand how many of the resistance substitutions act as they often occur far from Ser-130. Here, three IRT structures, TEM-30 (R244S), TEM-32 (M69I/M182T), and TEM-34 (M69V), are determined by x-ray crystallography at 2.00, 1.61, and 1.52 Å, respectively. In TEM-30, the Arg-244 → Ser substitution (7.8 Å from Ser-130) displaces a conserved water molecule that usually interacts with the β-lactam C3 carboxylate. In TEM-32, the substitution Met-69 → Ile (10 Å from Ser-130) appears to distort Ser-70, which in turn causes Ser-130 to adopt a new conformation, moving its Oγ further away, 2.3 Å from where the inhibitor would bind. This substitution also destabilizes the enzyme by 1.3 kcal/mol. The Met-182 → Thr substitution (20 Å from Ser-130) has no effect on enzyme activity but rather restabilizes the enzyme by 2.9 kcal/mol. In TEM-34, the Met-69 → Val substitution similarly leads to a conformational change in Ser-130, this time causing it to hydrogen bond with Lys-73 and Lys-234. This masks the lone pair electrons of Ser-130 Oγ, reducing its nucleophilicity for cross-linking. In these three structures, distant substitutions result in accommodations that converge on the same point of action, the local environment of Ser-130.

TEM-1 β-lactamase is the predominant source of resistance to β-lactams, such as the penicillins. TEM-1 and related class A β-lactamases confer resistance by hydrolyzing the β-lactam ring of these antibiotics; bacteria expressing these enzymes have become widespread in hospitals and in the community. Beginning in 1980s, three mechanism-based class A β-lactamase inhibitors, clavulanate, tazobactam, and sulbactam, have been used in combination with conventional penicillins to reverse this resistance (Fig. 1, *A–C*). However, since 1992, more than 26 so-called inhibitor-resistant TEM (IRT)[1] mutants have been selected, reversing susceptibility to these three mechanism-based inhibitors in the clinic (www.lahey.org/studies/temtable.stm) (1, 2).

The inhibition mechanisms of these three inhibitors are similar, involving a secondary cross-linking reaction after the initial primary nucleophilic attack by the enzyme on the β-lactam ring (Fig. 2) (3–7). The mechanism of inhibition has been studied kinetically (6, 8–14), by crystallography (4, 15), by simulation (10, 11, 16), and by mass spectrum analysis (5, 7) and is well understood (Fig. 2). The mechanism is thought to involve 8–10 different intermediates with the inactivation pathway (intermediate **2** → **4**) branching from conventional acyl intermediate hydrolysis (3–7). All three inhibitors ultimately form a covalent cross-link between Ser-70 and Ser-130. This latter residue is attacked by the reactive intermediate **2**, which can, alternatively, be hydrolyzed to give intermediate **3**, using the hydrolytic pathway (Fig. 2) (3–7). The inactivation and hydrolytic pathways compete during each reaction cycle. Although the hydrolytic pathway is over 100-fold faster than the inactivation pathway (3, 8, 9), inactivation is irreversible, and the enzyme is eventually completely inhibited.

The IRT enzymes that have been selected involve substitutions to several different residues. Some, such as S130G (TEM-76), are simple to understand: the cross-linking residue is simply replaced. Others, such as substitutions to Met-69, Trp-165, Met-182, Arg-244, Arg-275, and Asn-276 (17), are often distant from Ser-130, as far as 20 Å, making them harder to comprehend based on the wild type (WT) structure alone. Extensive site-directed mutagenesis and kinetic studies have been carried out on these mutant enzymes (see reviews by Chaibi *et al.* (17), Knox (18), and Yang *et al.* (19)). Although several molecular modeling studies of IRTs have been undertaken (6, 10), an atomic resolution structure is only available for one of them, TEM-84 (N276D) (20). To further explore the structural bases of resistance to inhibition, the structures of TEM-30 (R244S), TEM-32 (M69I/M182T), and TEM-34 (M69V) were determined by x-ray crystallography. These structures reveal a subtle set of accommodations that, in different ways, all end up disrupting the local environment of the cross-linking residue, Ser-130, while leaving the hydrolytic mechanism less affected.

MATERIALS AND METHODS

Enzyme Preparation—Site-directed mutagenesis was carried out using a modified two-step PCR protocol (21, 22). TEM-30, TEM-32, and TEM-34 were expressed and purified in a procedure modified from Dubus *et al.* (23). The protein was produced at room temperature in 2×

[1] The abbreviations used are: IRT, inhibitor-resistant TEM β-lactamase; WT, wild type; WT*, TEM M182T, a thermostable iso-functional mutant.
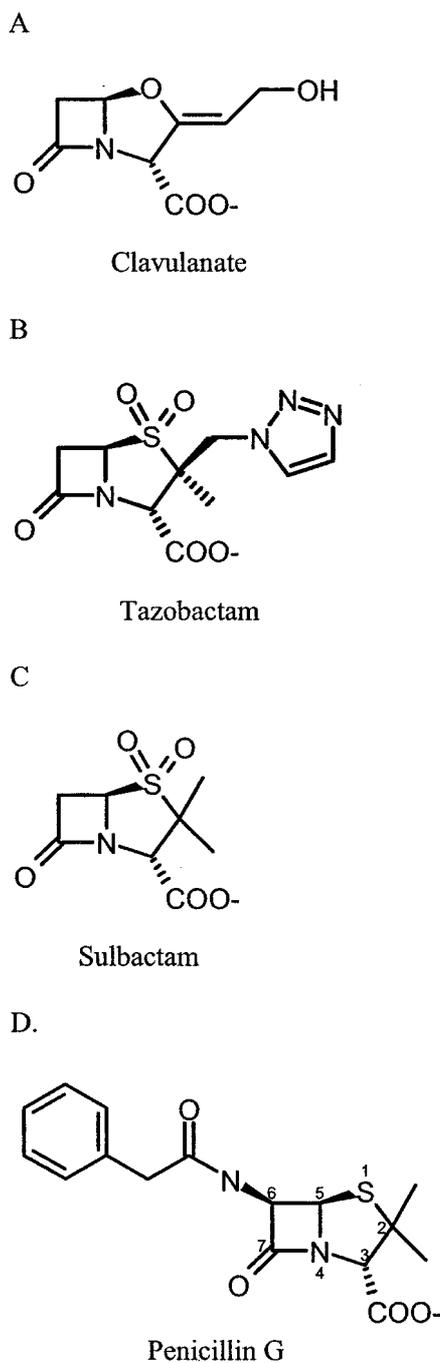
A

Clavulanate

B

Tazobactam

C

Sulbactam

D.

Penicillin G

FIG. 1. **Chemical structures of class A β-lactamase inhibitors (*A–C*) and penicillin G (*D*).** The numbering scheme shown for the penicillin G structure is also used in discussing the three mechanism-based inhibitors.

YT medium. Cells were collected by centrifugation and resuspended in 5 mM Tris/HCl, pH 8.0, containing 1 mM EDTA and 20% (w/v) sucrose in room temperature for 10 min. Cells were then collected and resuspended in ice-cold 5 mM MgCl$_2$ for 10 min. The supernatant was saved as the periplasmic contents, concentrated to about 100 ml, and dialyzed against 5 mM Tris/HCl, pH 8.0. The crude extract was applied to a Q-Sepharose Fast Flow column (Amersham Biosciences) equilibrated with 5 mM Tris/HCl, pH 8.0. The column was then washed extensively with 5 mM Tris/HCl, pH 8.0. The enzyme was eluted by 5 mM Tris/HCl, pH 8.0, containing 100 mM NaCl. The active fractions were pooled and dialyzed against 100 mM sodium P$_i$, pH 8.0. The protein was then applied to a Ni^{2+}-nitrilotriacetate-agarose column (Qiagen, Valencia, CA) equilibrated in the same buffer. The enzyme was eluted by 40 mM imidazole. The enzyme solution was concentrated to 6 mg/ml and stored in 200 mM potassium P$_i$, pH 7.0, 50% glycerol at −20 °C.

Thermal Denaturation—The enzyme was denatured by raising the temperature in 0.1 °C increments at a ramp rate of 2 °C/min in 200 mM potassium P$_i$, pH 7.0, using a Jasco 715 spectropolarimeter with a Peltier effect temperature controller and an in-cell temperature monitor (22). Denaturation was marked by an obvious transition in both the far-UV CD (223 nm) and fluorescence signals (maximum at 340 nm measured using a 300-nm cut-on filter). Both fluorescence and CD signals were monitored simultaneously. All melts were reversible and apparently two-state (22, 24). Temperature of melting (Tm) and van't Hoff enthalpy of unfolding (ΔH$_{VH}$) values were calculated using EXAM (25). The free energy of unfolding relative to WT was calculated using the method proposed by Becktel and Schellman (26): ΔΔG$_u$ = ΔTm·ΔS$_u^{WT}$ (26). A positive value of ΔΔG$_u$ indicates a stability gain, and a negative value indicates stability loss. The ΔS$_u^{WT}$ was 0.43 ± 0.02 kcal/mol·K.

Crystallization, Data Collection, and Refinement—TEM-30, TEM-32, and TEM-34 were crystallized using the hanging drop vapor diffusion technique, equilibrating an 8-μl droplet containing 5 mg/ml protein and 0.65 M sodium potassium P$_i$ buffer, pH 8.0, against a reservoir solution of 0.75 ml of 1.4 M sodium potassium P$_i$ buffer, pH 8.0 (22). Droplets were initially seeded with microcrystals of the TEM mutant M182T (27). Crystals were cryoprotected by 25% sucrose in 1.6 M potassium P$_i$ buffer, pH 8.0.

Crystals were mounted in a nylon loop and flash-frozen in liquid nitrogen (100 K). X-ray diffraction data were collected on the 5-ID beamline (λ = 1.0000 Å) of the DuPont-Northwestern-Dow Collaborative Access Team (DND-CAT) at the Advanced Photon Source (Argonne, IL) using a MARCCD detector. Data were processed and merged using the DENZO/SCALEPCK suite (28). The M182T structure (Protein Data Bank accession number 1JWP (22)) was used as an initial model for molecular replacement. After rigid body refinement and torsion angle annealing using CNS (29), mutated residues were fit into $F_o − F_c$ difference density maps. The models were refined by cycles of Cartesian and B-factor refinement (30) followed by manual corrections using the program Turbo (31).

RESULTS

In the following discussion, we compare the IRT structures with that of a laboratory variant of TEM-1, TEM M182T, which is kinetically and structurally nearly identical to TEM-1 (22). We will refer to this enzyme, M182T, as WT*. We use WT* as a point of comparison for the IRT enzymes for several reasons. First, we have ourselves determined the structure of WT* in the same buffer, space group, and cryo-conditions as for the IRT mutants. We also have refined WT* and the IRTs using the same protocols. This reduces small crystallographic differences that could otherwise occur when comparing the IRT structures with "true" WT, determined previously in other laboratories (32–35). Second, WT* is 2.5 kcal/mol more stable than TEM-1 (22). This higher stability makes it express (36, 37), crystallize, and diffract better than WT TEM-1 such that we have determined its structure to a 0.85-Å resolution (38). We note that such stable iso-functional mutants are often used as pseudo-wild type in other enzymes, such as lysozyme (39). Moreover, many reported TEM-1 wild type structures derive from the Bluescript plasmid (32–35) and contain two substitutions, Ile-84 → Val and Val-182 → Ala, relative to WT TEM-1 found in clinical isolates.

The substitution Met-182 → Thr, which occurs in TEM-32, takes place over 15 Å from the active site. This substitution has been shown to be a "global stabilizer" in extended spectrum β-lactamase mutants (27, 36). To investigate the effects on enzyme stability of this substitution and its coupling to the IRT substitution Met-69 → Ile and Met-69 → Leu, the relative thermostabilities of M69I/M182T (TEM-32), M69L (TEM-33), M69V (TEM-34), and M69I (TEM-40) were determined by reversible, two-state denaturation (22) and analyzed for the change in free energy of folding using the method of Becktel and Schellman (26). When compared with WT, M69I and M69V are 2.9 and 0.3 °C (1.3 and 0.1 kcal/mol) less stable than WT, respectively (Fig. 3). On the other hand, M69L is 2.3 °C (1.0 kcal/mol) more stable than WT. The perturbation of stability by
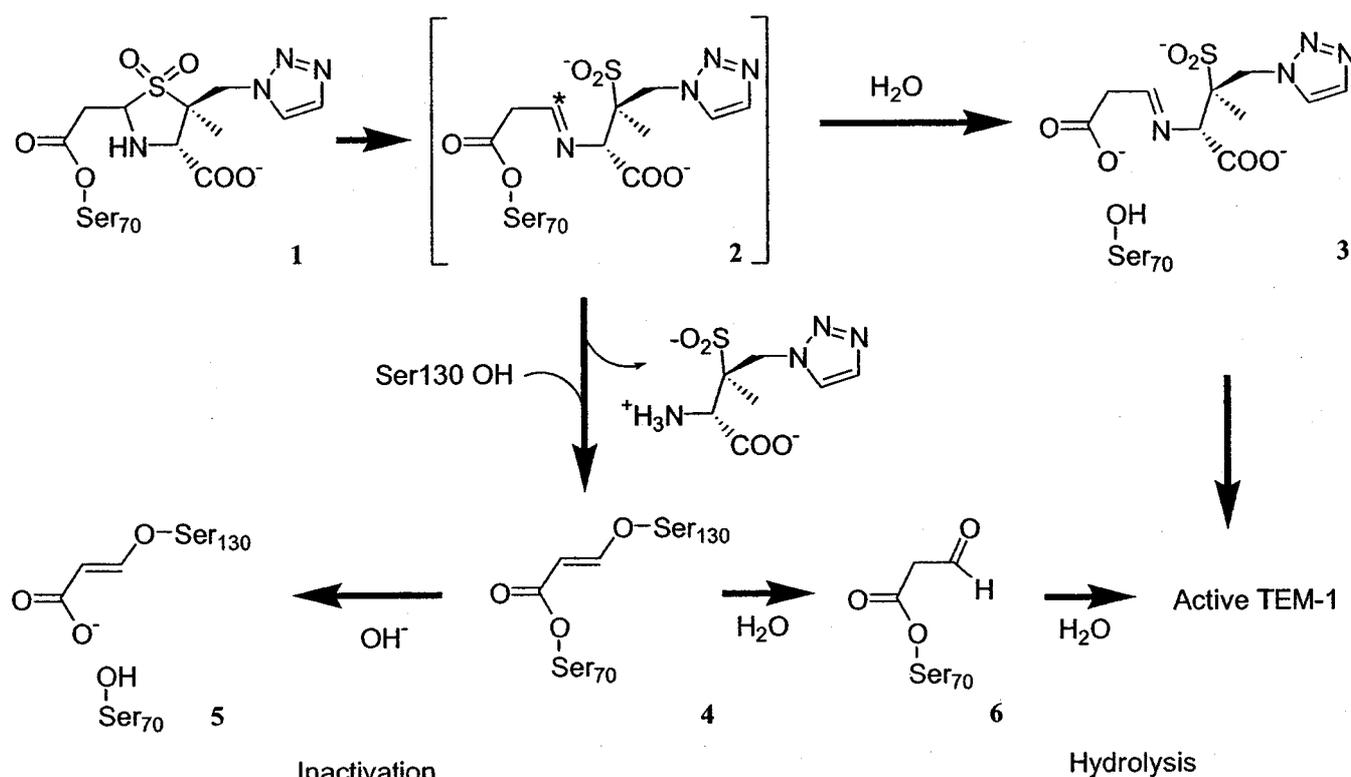
FIG. 2. **Simplified mechanism of TEM-1 inhibition by tazobactam.** The scheme is adapted from Kuzin *et al.* (4).
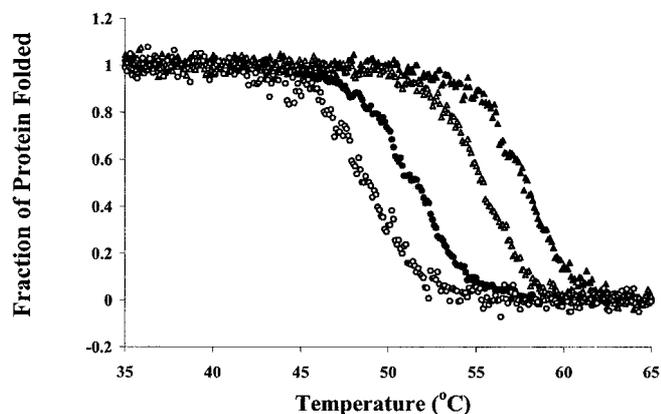

FIG. 3. **Representative thermal denaturation curves.** *Solid circles*, WT; *solid triangles*, WT*; *open circles*, TEM-40 (M69I); and *open triangles*, TEM-32 (M69I/M182T).

the different Met-69 mutants is qualitatively consistent with the modeling studies by Labia and colleagues (10). TEM-32 (M69I/M182T) is 3.7 °C (1.6 kcal/mol) more stable than WT but 2.4 °C (1.3 kcal/mol) less stable than WT* (Fig. 3).

Crystallographic structures of TEM-30 (R244S), TEM-32 (M69I/M182T), and TEM-34 (M69V) were determined at 2.00-, 1.61-, and 1.52-Å resolution, respectively (Table I). The WT* structure (Protein Data Bank accession number 1JWP (22)) was used as an initial model. For all three structures, the unit cell parameters are similar to WT* (Table I). After rigid body refinement and torsion angle annealing in CNS (29), substituted residues were fit into the $F_o - F_c$ difference density maps. Several rounds of Cartesian and B-factor refinement resulted in models with final R-factors and R_{free} values of 17.6 and 21.2%, 19.7 and 21.7%, and 17.7 and 18.9% for TEM-30, TEM-32, and TEM-34, respectively. All three structures closely resemble the WT* structure with root mean square deviation of all Cα atoms of 0.28, 0.41, and 0.30

Å for TEM-30, TEM-32, and TEM-34, respectively. The stereochemistry of the models was evaluated by the program Procheck (40). All residues except Leu-220, Ile-69 in TEM-32, and Val-69 in TEM-34 were in the most favored region of the Ramachandran plot, and Leu-220, Ile-69 in TEM-32, and Val-69 in TEM-34 were in the additionally allowed region.

In the TEM-30 structure, two water molecules, Wat63 and Wat139, were modeled into the cavity created by the Arg-244 → Ser substitution using an $F_o - F_c$ electron density map (Fig. 4A). With the exception of the Arg-244 → Ser substitution, other catalytic residues are located in positions similar to those seen in WT* (Table II). On the other hand, the well ordered water that is observed to hydrogen bond to Arg-244 in most WT structures (*e.g.* Wat294 in Protein Data Bank accession number structure 1FQG (34)) is *not* observed in the TEM-30 structure (Fig. 5A).

In the TEM-32 and TEM-34 structures, Met-69 is substituted to isoleucine and valine, respectively, and these residues were fit into $F_o - F_c$ electron density maps (Fig. 4, *B–D*). Most active site residues in TEM-32 and TEM-34 are in locations similar to those seen in WT* (Table II). There are two exceptions to this: in TEM-32, Ser-130, which has a major role in reacting with inhibitors (Fig. 2), adopts a different conformation in the active site, rotating by 64° about χ_1 (Fig. 5B). In TEM-34, Ser-130 rotates by 27° about χ_1 (Fig. 5C). In both TEM-32 and TEM-34, two conformations of catalytic residue Ser-70 were modeled based on $F_o - F_c$ electron density maps (Fig. 4, *C* and *D*). When only the canonical conformation of Ser-70 was modeled, the B-factor of the Ser-70 Oγ atom was twice as high as that of the Ser-70 Cβ, which is, in turn, in the range of those of nearby residues (data not shown). Also, a positive electron density peak was observed adjacent to the canonical position of the Oγ, and a negative peak was observed overlapping the canonical position, consistent with two conformations of Ser-70 being present (Fig. 4C).

TABLE I
Data processing and refinement statistics

	TEM-30	TEM-32	TEM-34
Unit cell parameters (a, b, c, (Å))	41.53, 59.67, 88.10	41.22, 60.50, 88.71	41.37, 59.60, 88.29
Resolution range for refinement	17.0–2.00	17.0–1.61	17.0–1.52
(Å)	(2.07–2.00)[a]	(1.67–1.61)	(1.57–1.52)
Unique reflections	14,828	29,385	34,443
Total observations	75,684	181,694	208,926
R_{merge} (%)	8.8 (34.2)	6.1 (27.3)	5.4 (34.5)
Completeness (%)	96.4 (98.4)	99.2 (99.8)	99.7 (100)
$\langle I \rangle / \langle \sigma(I) \rangle$	16.6 (3.6)	24.6 (6.1)	29.5 (4.7)
Number of protein residues	263	263	263
Number of ions	1 HPO_4^{2-}	1 HCO_3^-, 2 K^+	2 HPO_4^{2-}, 1 K^+
Number of water molecules	224	328	398
r.m.s.d.[c] bond lengths (Å)	0.009	0.009	0.009
r.m.s.d. bond angles (°)	1.5	1.6	1.5
R-factor (%)	17.6	19.7	17.7
R_{free} (%)[b]	21.2	21.7	18.9

[a] Values in parentheses are for the highest resolution shell.

[b] R_{free} was calculated with 10% of reflections set aside randomly.

[c] r.m.s.d., root mean square deviation.

FIG. 4. **Simulated annealing omit electron density maps, contoured at 2.5 σ (A, B, and D), as well as an overlay of $2F_o - F_c$ and $F_o - F_c$ electron density maps (C), in the regions where the major changes are observed in the mutant enzymes.** Carbon, nitrogen, oxygen, and sulfur atoms are colored *yellow*, *blue*, *red*, and *green*, respectively. *A*, TEM-30 in the Ser-244 region. *B*, TEM-32 in the Ser-130 region. *C*, $2F_o - F_c$ electron density map (*blue* at 1.0 σ) and $F_o - F_c$ electron density map (*green* at 2.0 σ and *red* at −2.0 σ) in the Val-69 and Ser-70 region of TEM-34 before multiple conformations of Ser-70 were modeled. The stick model represents the final model of TEM-34. *D*, TEM-32 in the Ile-69 and Ser-70 region. Space group was P2$_1$2$_1$2$_1$ for all crystals.
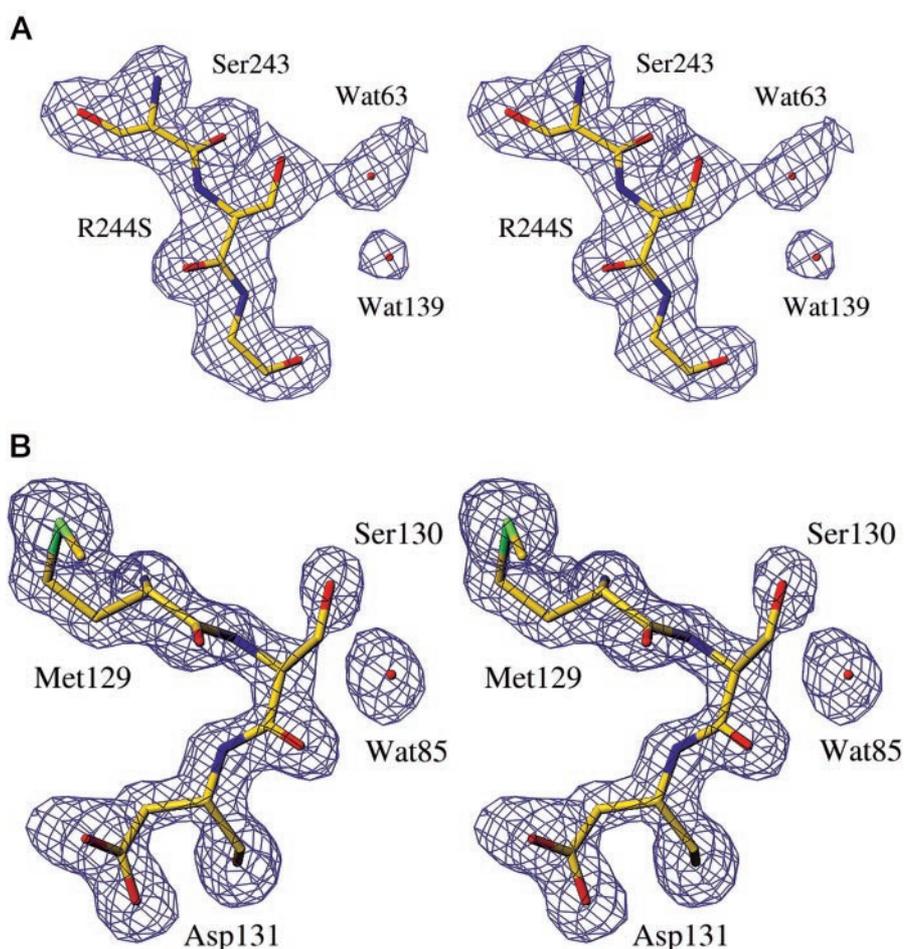
DISCUSSION

IRT enzymes must at once diminish the apparent affinity of mechanism-based inhibitors, such as clavulanate, while maintaining enough activity against conventional (substrate) antibiotic β-lactams, such as penicillin, to confer resistance to bacteria that express them. This would seem tricky since the mechanism-based inhibitors are themselves β-lactams, resemble the substrates, and bind to most of the same catalytic residues. Thus, to be an effective IRT, a mutant must disrupt the part of the mechanism that leads to irreversible inhibition but leave the fundamental hydrolytic aspect of the β-lactamase relatively intact. In the structures of the three IRT enzymes

TEM-30, TEM-32, and TEM-34, we observe three subtle, but nevertheless crucial, accommodations that serve this end. Although the residue substitutions in these three mutant enzymes, and indeed in the previously determined TEM-84 (20), are distant from Ser-130, they all act to disrupt the local environment in the region of this residue.

The Loss of a Conserved Water Molecule Confers Inhibitor Resistance in TEM-30—TEM-30 achieves its IRT status through the substitution Arg-244 → Ser. Although this residue is highly conserved in class A β-lactamases (41), it is relatively distant from Ser-130; at their closest, the two residues are 7.8 Å apart. In TEM-1, Arg-244 makes two hydrogen bonds with
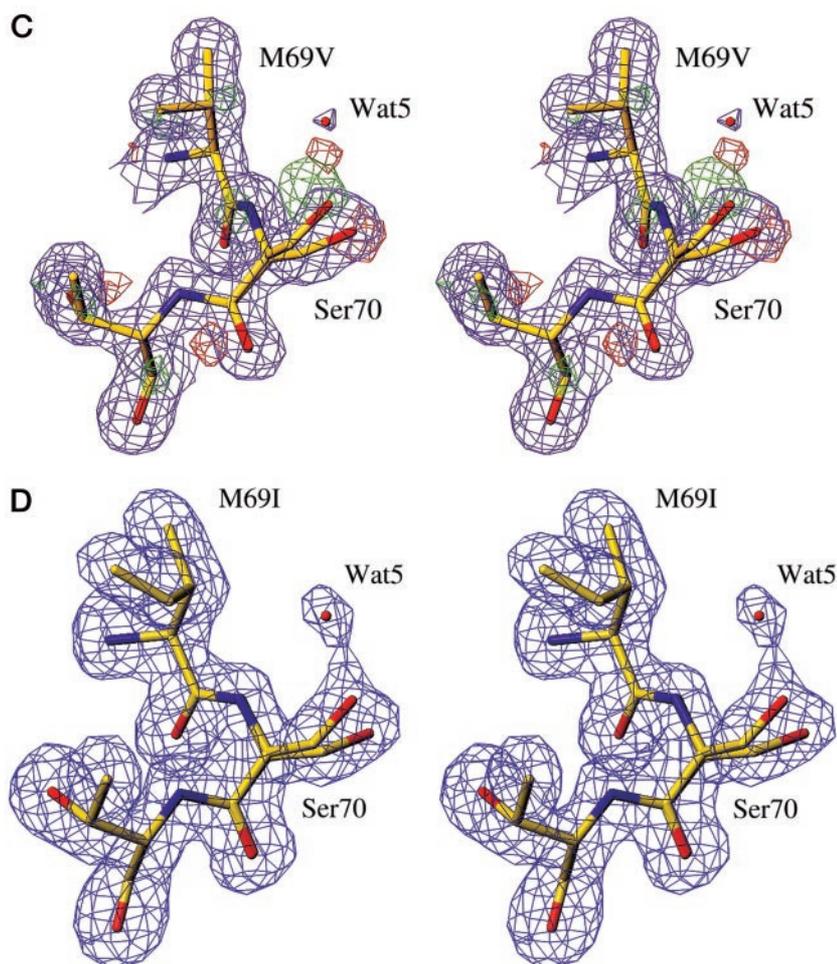
FIG. 4—*continued*

TABLE II
Selected distances in TEM-30, TEM-32, and TEM-34 as compared with WT*

	Distance			
	TEM-30	TEM-32	TEM-34	WT*[a]
	Å	Å	Å	Å
Catalytic water[b], Ser-70 Oγ	2.9	2.8	2.7	2.8
Catalytic water, Glu-166 Oε2	2.4	2.5	2.5	2.7
Catalytic water, Asn-170 Nδ	2.7	2.7	2.6	2.6
Oxyanion hole water[c], Ser-70 Oγ	2.8	3.0	2.8	2.7
Oxyanion hole water, Ser-70 N	2.7	2.9	3.1	2.8
Oxyanion hole water, Ala-237 N	3.0	3.2	3.0	3.1
Oxyanion hole water, Ala-237 O	2.9	2.6	2.4	2.8
C3 water[d], Arg-244 NH1	NP[e]	2.9	2.9	2.8
C3 water, Ser-235 Oγ	NP	3.1	2.9	2.8
Ser-70 Oγ, Lys-73 Nζ	2.8	3.1	3.2	2.8
Ser-70 Oγ, Ser-130 Oγ	3.5	5.5	3.1	3.2
Ser-70 Oγ(B)[f], Lys-73 Nζ	NP	4.3	4.1	NP
Ser-70 Oγ(B), Ser-130 Oγ	NP	5.5	3.4	NP
Ser-130 Oγ, Lys-73 Nζ	4.2	5.4	3.2	3.8
Ser-130 Oγ, Lys-234 Nζ	2.5	3.3	2.8	2.8
Lys-73 Nζ, Asn-132 Oδ1	3.0	3.0	2.9	3.0

[a] PDB 1JWP (27).
[b] The catalytic water is numbered Wat6 in TEM-30, TEM-32, and TEM-34, and Wat57 in WT*.
[c] The oxyanion hole water is numbered Wat5 in TEM-30, TEM-32, and TEM-34, and Wat196 in WT*.
[d] This water, expected to interact with C3 carboxylate of β-lactam, is numbered Wat7 in TEM-32 and TEM-34, and Wat99A in WT*.
[e] Not present.
[f] Measured from the alternative conformations seen in TEM-32 and TEM-34.

Asn-276 (34). A conserved water molecule is anchored by the guanidinium group of Arg-244 and the backbone carbonyl group of Val-216. In the penicillin G acyl complex (Protein Data Bank accession number 1FQG (34)), this water molecule interacts with C3 carboxylate group of the β-lactam (Figs. 1*D* and 5*A*). Structural and mutagenesis studies on Arg-244 suggest

that it contributes to ligand binding throughout the reaction cycle by stabilizing the C3 carboxylate group of the substrate (14, 42). Replacing Arg-244 with residues that have shorter side chains, *e.g.* serine in TEM-30 or cysteine in TEM-31, results in reduced hydrolysis of penicillin but increased resistance to all three mechanism-based inhibitors (10, 12, 14). On
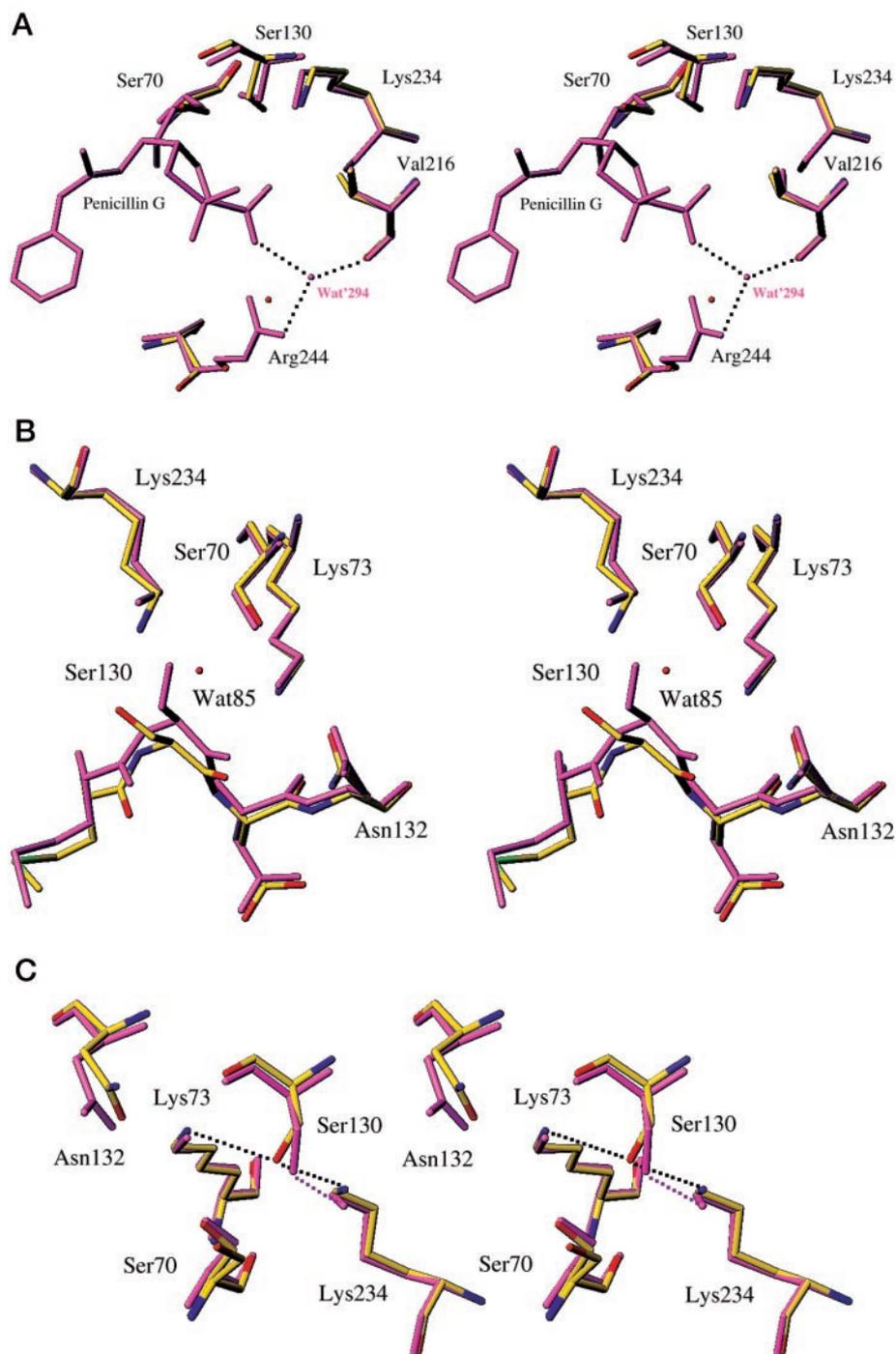
FIG. 5. **Comparing the IRT mutant structure with that of WT and WT* TEM-1.** Mutant structures are colored as in Fig. 4. *A*, comparison of the C3 carboxylate region of the penicillin G complex structure (*purple*, Protein Data Bank accession number 1FQG (34)) and of TEM-30. Water 294 in the acyl complex structure is labeled as *Wat'294*. The three hydrogen bond interactions observed in the penicillin G acyl complex structure are represented as *dashed lines*. *B*, stereo view of the superposition of the Ser-130 region of TEM-32 and WT* (*purple*). *C*, stereo view of the superposition of the Ser-130 regions of TEM-34 and WT* (*purple*). The *dashed lines* represented the hydrogen bond interactions between Ser-130, Lys-73, and Lys-234.

the other hand, this same water molecule is thought to activate the opening of the five-membered ring of clavulanate, which is a key step in the inactivation pathway (6).

In TEM-30, this conserved water disappears (Fig. 5*A*). The loss of this water should reduce the binding affinity of inhibitors and allow the reactive Schiff base of the inhibitors (Fig. 2) to swing away from Ser-130 since the proximal anchor point of the inhibitor at the C3 carboxylate, the water, has been lost. Although the hydrolysis pathway is also affected by this perturbation, the inhibition reaction is affected even more strongly (17). This differential effect seems sensible given the proximity of the perturbation to the group on the inhibitor with which Ser-130 is meant to react. These observations are consistent with the previously determined structure of TEM-84 (N276D, Protein Data Bank accession number 1CK3 (20)) in which this

same conserved water is thought to be only transiently present based on its low crystallographic occupancy. In TEM-84, the Asn-276 → Asp substitution is thought to reduce the electrostatic interaction between this water molecule and Arg-244, whose positive charge will be shielded by the negative charge of Asp-276 to which Arg-244 hydrogen bonds.

The Conformation of Ser-130 Changes in TEM-32 and TEM-34—In TEM-32, the substitution Met-69 → Ile, which is 10.0 Å from Ser-130, distorts the canonical conformation of Ser-70. This distortion is manifested in the two conformations that Ser-70 adopts in TEM-32, one a canonical conformation typical of apo-TEM enzymes and the other a new, apparently higher energy conformation rotated about χ_1. The alternative conformation of Ser-70 is also observed in TEM-34 (below). We originally wondered whether this new conformational sampling on

the part of the catalytic nucleophile might contribute to inhibitor resistance, for instance by acting as a lever arm that disrupts the position of the Schiff base of intermediate *2* (Fig. 2), which is attacked by Ser-130 in the cross-linking reaction. Although we cannot rule out a direct effect on inhibition due to this conformational sampling by Ser-70, we could not find a simple mechanism by which this might lead to inhibitor resistance. Instead, the effect on Ser-70 appears to be transmitted to Ser-130, with which it normally hydrogen bonds, resulting in Ser-130 adopting a new conformation (Fig. 5*B*). In this new conformation, the χ_1 angle of Ser-130 changes by 64º, moving the Oγ 2.3 Å away from the canonical Oγ of Ser-70. In this conformation, the Oγ of Ser-130 is 5.5 and 5.4 Å from the Oγ of Ser-70 and the Nζ of Lys-73, respectively, as compared with 3.2 and 3.8 Å in WT* (Fig. 5*B* and Table II). Also, a new water molecule (Wat85) appears between Ser-130 and Ser-70 (Figs. 4*B* and 5*B*). The movement of the Oγ of Ser-130, which is the ultimate covalent attachment point for the inhibitors (Fig. 2), provides a simple explanation of inhibitor resistance in TEM-32. Indeed, such a mechanism is conceptually similar to that invoked by other IRT substitutions such as Ser-130 → Gly (TEM-76), where the Oγ is simply deleted. Ser-130 also plays a role in the hydrolysis of substrate β-lactams, partly by acting in a network of interactions that act as the catalytic acid in the nucleophilic attack on the β-lactam by the enzyme. In TEM-32, this role will presumably be disrupted, consistent with the loss of catalytic efficiency, in which k_{cat} drops by 5-fold (11, 17). Here again, the modest loss in intrinsic activity is more than offset by the loss in inhibition rate constant because of the effect on a group intimately involved with the latter.

The second substitution that TEM-32 contains is Met-182 → Thr, which is 20.5 Å from Ser-130 and has no obvious connection of any kind with the active site. Met-182 → Thr occurs in clinical isolates in combination with other substitutions in β-lactamase mutant enzymes but never has been found alone in clinical isolates. Palzkill and colleagues (36, 43) have shown that this substitution leads to higher expression levels of the mutant enzymes that contain it. We have found that this substitution dramatically stabilizes TEM enzymes thermodynamically, only occurs in mutants that would otherwise be destabilized relative to the WT enzyme, and has no significant effect on enzyme activity (27). True to this pattern, the Met-69 → Ile substitution destabilized TEM-32 relative to TEM-1 by 2.9 °C (1.3 kcal/mol) (Fig. 3), but Met-182 → Thr restabilizes M69I by 6.6 °C (2.9 kcal/mol). The reason why this distant substitution is selected is that it restabilizes the enzyme against the insult incurred by the gain-of-function substitution, Met-69 → Ile. Consistent with this view, IRT substitutions that do not significantly destabilize the enzymes, such as M69L (TEM-33) or M69V (TEM-34), whose stability is almost identical to or greater than that of TEM-1, are not observed to occur with Met-182 → Thr.

In TEM-34 (M69V), as in TEM-32, the substitution at Met-69 leads to a conformational change in Ser-130, again apparently through a perturbation in Ser-70, which, as in TEM-32, adopts a second conformation. In this new conformation of Ser-130, which differs not only from that adopted in WT* but also from that adopted in TEM-32, the Oγ of Ser-130 moves 0.3 Å away from the Oγ of Ser-70 but 0.6 Å closer to the Nζ of Lys-73 (Table II). In this conformation, Ser-130 Oγ forms hydrogen bonds with both Lys-73 Nζ (3.2 Å) and Lys-234 Nζ (2.8 Å), as compared with hydrogen bonding with Lys-234 Nζ (2.8 Å) alone in WT* (Fig. 5*C* and Table II). These hydrogen bonds in TEM-34 thus orient the lone pair electrons on the Ser-130 Oγ toward the Nζ amino groups of the two lysines. We therefore expect this to reduce the ability of Ser-130 to attack the Schiff base in

the inhibitor acyl intermediate *2* (Fig. 2) since both of the potentially nucleophilic lone pairs are tied up in hydrogen bonds. As compared with TEM-1, where only one lone pair is used in a lysine hydrogen bond, the rate of cross-linking should be reduced, and inhibition should be attenuated. We note that in the acyl-enzyme complex between TEM-1 and penicillin G, both lysines hydrogen bond with Ser-130; this hydrogen bonding pattern is thus not in itself unprecedented. However, the preformation of both hydrogen bonds in the apo-enzyme suggests that these interactions will be stronger in TEM-34, making the Ser-130 Oγ less able to reorient to act as the cross-linking nucleophile.

Conclusion—Under the pressure of mechanism-based inhibitors, mutant TEM β-lactamases that avoid covalent cross-linking have been selected. The simplest way they might do this, and the way a protein engineer might first try, is through substitutions to Ser-130 itself. Indeed, evolution has explored such substitutions in clinically isolated mutant enzymes such as TEM-59, TEM-76, and TEM-89. More substitutions have been explored at positions such as Met-69, Met-182, Arg-244, Asn-276 (17–19), which are relatively distant from Ser-130. At first glance, these distant substitutions are difficult to understand, as indeed are similarly distant resistance substitutions in other antimicrobial targets, such as HIV-1 protease (44). With the structures of TEM-30, TEM-32, and TEM-34 and the previously determined structure of TEM-84 (20), the bases of inhibitor resistance in class A β-lactamases become comprehensible.

All four mutant enzymes perturb the local environment of Ser-130, the point of cross-linking. The way they perturb this region differs for each enzyme, and the perturbations are transmitted over some distance. In this sense, the structural origins of resistance can be subtle. Substitutions such as Arg-244 → Ser (TEM-30) and Asn-276 → Asp (TEM-84) (20) displace a structural water that organizes the substrate in the region of Ser-130. Substitutions at Met-69 (TEM-32 and TEM-34) lead to conformational changes in Ser-130 that attenuate cross-linking. At atomic resolution, these disparate and distant resistance substitutions focus their effects on the same local region, that of Ser-130, providing a common logic for inhibitor resistance. These structures may provide starting points for the design of novel inhibitors to combat these increasingly widespread resistance enzymes.

REFERENCES

1. Blazquez, J., Baquero, M. R., Canton, R., Alos, I., and Baquero, F. (1993) *Antimicrob. Agents Chemother.* **37,** 2059–2063
2. Belaaouaj, A., Lapoumeroulie, C., Canica, M. M., Vedel, G., Nevot, P., Krishnamoorthy, R., and Paul, G. (1994) *FEMS Microbiol. Lett.* **120,** 75–80
3. Knowles, J. R. (1985) *Acc. Chem. Res.* **18,** 97–104
4. Kuzin, A. P., Nukaga, M., Nukaga, Y., Hujer, A., Bonomo, R. A., and Knox, J. R. (2001) *Biochemistry* **40,** 1861–1866
5. Yang, Y., Janota, K., Tabei, K., Huang, N., Siegel, M. M., Lin, Y. I., Rasmussen, B. A., and Shlaes, D. M. (2000) *J. Biol. Chem.* **275,** 26674–26682
6. Imtiaz, U., Billings, E. M., Knox, J. R., Manavathu, E. K., Lerner, S. A., and Mobashery, S. (1993) *J. Am. Chem. Soc.* **115,** 4435–4442
7. Brown, R. P., Aplin, R. T., and Schofield, C. J. (1996) *Biochemistry* **35,** 12421–12432
8. Fisher, J., Charnas, R. L., and Knowles, J. R. (1978) *Biochemistry* **17,** 2180–2184
9. Charnas, R. L., and Knowles, J. R. (1981) *Biochemistry* **20,** 3214–3219
10. Chaibi, E. B., Peduzzi, J., Farzaneh, S., Barthelemy, M., Sirot, D., and Labia, R. (1998) *Biochim. Biophys. Acta* **1382,** 38–46
11. Delaire, M., Labia, R., Samama, J. P., and Masson, J. M. (1992) *J. Biol. Chem.* **267,** 20600–20606
12. Bret, L., Chaibi, E. B., Chanal-Claris, C., Sirot, D., Labia, R., and Sirot, J.

(1997) *Antimicrob. Agents Chemother.* **41,** 2547–2549

13. Bush, K., Macalintal, C., Rasmussen, B. A., Lee, V. J., and Yang, Y. (1993) *Antimicrob. Agents Chemother.* **37,** 851–858
14. Zafaralla, G., Manavathu, E. K., Lerner, S. A., and Mobashery, S. (1992) *Biochemistry* **31,** 3847–3852
15. Chen, C. C., and Herzberg, O. (1992) *J. Mol. Biol.* **224,** 1103–1113
16. Imtiaz, U., Manavathu, E. K., Mobashery, S., and Lerner, S. A. (1994) *Antimicrob. Agents Chemother.* **38,** 1134–1139
17. Chaibi, E. B., Sirot, D., Paul, G., and Labia, R. (1999) *J. Antimicrob. Chemother.* **43,** 447–458
18. Knox, J. R. (1995) *Antimicrob. Agents Chemother.* **39,** 2593–2601
19. Yang, Y., Rasmussen, B. A., and Shlaes, D. M. (1999) *Pharmacol. Ther.* **83,** 141–151
20. Swaren, P., Golemi, D., Cabantous, S., Bulychev, A., Maveyraud, L., Mobashery, S., and Samama, J. P. (1999) *Biochemistry* **38,** 9570–9576
21. Ho, S. N., Hunt, H. D., Horton, R. M., Pullen, J. K., and Pease, L. R. (1989) *Gene (Amst.)* **77,** 51–59
22. Wang, X., Minasov, G., and Shoichet, B. K. (2002) *Proteins* **47,** 86–96
23. Dubus, A., Wilkin, J. M., Raquet, X., Normark, S., and Frere, J. M. (1994) *Biochem. J.* **301,** 485–494
24. Raquet, X., Vanhove, M., Lamotte-Brasseur, J., Goussard, S., Courvalin, P., and Frere, J. M. (1995) *Proteins* **23,** 63–72
25. Kirchoff, W. (1993) *EXAM: A Two-state Thermodynamic Analysis Program*, Gaithersburg, MD
26. Becktel, W. J., and Schellman, J. A. (1987) *Biopolymers* **26,** 1859–1877
27. Wang, X., Minasov, G., and Shoichet, B. K. (2002) *J. Mol. Biol.* **320,** 85–95
28. Otwinowski, Z., and Minor, W. (1997) *Methods Enzymol.* **276,** 307–326
29. Brünger, A. T., Adams, P. D., Clore, G. M., DeLano, W. L., Gros, P., Grosse-Kunstleve, R. W., Jiang, J. S., Kuszewski, J., Nilges, M., Pannu, N. S., Read, R. J., Rice, L. M., Simonson, T., and Warren, G. L. (1998) *Acta Crystallogr. Sect. D Biol. Crystallogr.* **54,** 905–921
30. Engh, R. A., and Huber, R. (1991) *Acta Crystallogr. Sect. A* **47,** 392–400
31. Cambillau, C., and Roussel, A. (1997) *Turbo Frodo*, OpenGL Ed., Universite Aix-Marseille II, Marseille, France
32. Short, J. M., Fernandez, J. M., Sorge, J. A., and Huse, W. D. (1988) *Nucleic Acids Res.* **16,** 7583–7600
33. Chaibi, E. B., Peduzzi, J., Barthelemy, M., and Labia, R. (1997) *J. Antimicrob. Chemother.* **39,** 668–669
34. Strynadka, N. C., Adachi, H., Jensen, S. E., Johns, K., Sielecki, A., Betzel, C., Sutoh, K., and James, M. N. (1992) *Nature* **359,** 700–705
35. Jelsch, C., Mourey, L., Masson, J. M., and Samama, J. P. (1993) *Proteins* **16,** 364–383
36. Huang, W., and Palzkill, T. (1997) *Proc. Natl. Acad. Sci. U. S. A.* **94,** 8801–8806
37. Farzaneh, S., Chaibi, E. B., Peduzzi, J., Barthelemy, M., Labia, R., Blazquez, J., and Baquero, F. (1996) *Antimicrob. Agents Chemother.* **40,** 2434–2436
38. Minasov, G., Wang, X., and Shoichet, B. K. (2002) *J. Am. Chem. Soc.* **124,** 5333–5340
39. Matsumura, M., and Matthews, B. W. (1989) *Science* **243,** 792–794
40. Laskowski, R. A., MacArthur, M. W., Moss, D. S., and Thornton, J. M. (1993) *J. Appl. Crystallogr.* **26,** 283–291
41. Ambler, R. P., Coulson, A. F., Frere, J. M., Ghuysen, J. M., Joris, B., Forsman, M., Levesque, R. C., Tiraby, G., and Waley, S. G. (1991) *Biochem. J.* **276,** 269–270
42. Moews, P. C., Knox, J. R., Dideberg, O., Charlier, P., and Frere, J. M. (1990) *Proteins* **7,** 156–171
43. Sideraki, V., Huang, W., Palzkill, T., and Gilbert, H. F. (2001) *Proc. Natl. Acad. Sci. U. S. A.* **98,** 283–288
44. Condra, J. H., Schleif, W. A., Blahy, O. M., Gabryelski, L. J., Graham, D. J., Quintero, J. C., Rhodes, A., Robbins, H. L., Roth, E., Shivaprakash, M., Titus, D., Yang, T., Squires, K. E., Deutsch, P. S., and Emini, E. A. (1995) *Nature* **374,** 569–571